GaAs-based superluminescent diodes with window-like facet structure for low spectral modulation at high output powers

2016 Semicond. Sci. Technol. 31 045003

(http://iopscience.iop.org/0268-1242/31/4/045003)

OPEN ACCESS
IOP Publishing
Semiconductor Science and Technology
Semicond. Sci. Technol. **31** (2016) 045003 (6pp)
doi:10.1088/0268-1242/31/4/045003

GaAs-based superluminescent diodes with window-like facet structure for low spectral modulation at high output powers

O M S Ghazal[1], D T Childs[1], B J Stevens[2], N Babazadeh[1], R A Hogg[1] and K M Groom[1]

[1] Department of Electronic & Electrical Engineering, The University of Sheffield, Nanoscience & Technology Building, North Campus, Broad Lane, Sheffield, S3 7HQ, UK
[2] EPSRC National Centre for III-V Technologies, Department of Electronic & Electrical Engineering, The University of Sheffield, Nanoscience & Technology Building, North Campus, Broad Lane, Sheffield, S3 7HQ, UK

E-mail: k.m.groom@sheffield.ac.uk

Received 2 November 2015, revised 5 January 2016
Accepted for publication 1 February 2016
Published 1 March 2016

Abstract

We demonstrate a GaAs-based superluminescent diode (SLD) based on the incorporation of a window-like back facet into a self-aligned stripe structure in order to reduce the effective facet reflectivity. This allows the realisation of SLDs with low spectral modulation depth (SMD) at high power spectral density (PSD), without the application of anti-reflection coatings to either facet. This approach is therefore compatible with ultra-broadband gain active elements. We show that 30 mW output power can be attained in a narrow bandwidth, corresponding to 2.2 mW nm^{-1} PSD with only 5% SMD, centred about 990 nm. We discuss the design criteria for high power and low SMD and the deviation from a linear dependence of SMD on output power, resulting from Joule heating in the self-aligned stripe.

Keywords: superluminescent diode, low reflectivity facets, semiconductor device fabrication

(Some figures may appear in colour only in the online journal)

Superluminescent diodes (SLDs) offer relatively high power over a broad and smooth emission spectrum. Their waveguide structure enables far higher brightness than light emitting diodes and efficient fibre coupling, useful in many applications such as fibre-optic gyroscopes and optical coherence tomography. A key parameter defining the coherence properties of the SLD is the spectral modulation depth (SMD), which occurs due to Fabry–Perot modes arising from non-zero reflection at the facets of the device. Current methods to suppress this reflection rely on the use of anti-reflection (AR) coatings, which work to directly decrease the facet reflectivity. However, ultra-low reflectivity is difficult to achieve over broad bandwidths. Presently 100 nm is routinely required and hundreds of nm is desirable. An alternative method to reduce the effective reflectivity (describing light coupled back into the waveguide) is an angled waveguide.

Tilted facets, in which SLD waveguides are mis-oriented to the crystal-axis by an angle (typically 5°–10°) from the normal to the cleaved facet, suppress back reflection by deflecting reflected light outside the waveguide. This allows an effective facet reflectivity, R_{eff}, as low as $\sim 10^{-4}$. This is further reduced to 10^{-5} when also combined with an AR coating [1]. Transparent (window) regions can provide typical $R_{eff} < 10^{-3}$ [2]. In a traditional window structure, the waveguide is terminated and light is allowed to spread in an un-pumped region prior to the cleaved facet such that only a small fraction of the light is re-coupled back into the waveguide following reflection at the cleaved facet. Windows are inherently broad-band and can be combined with AR coatings

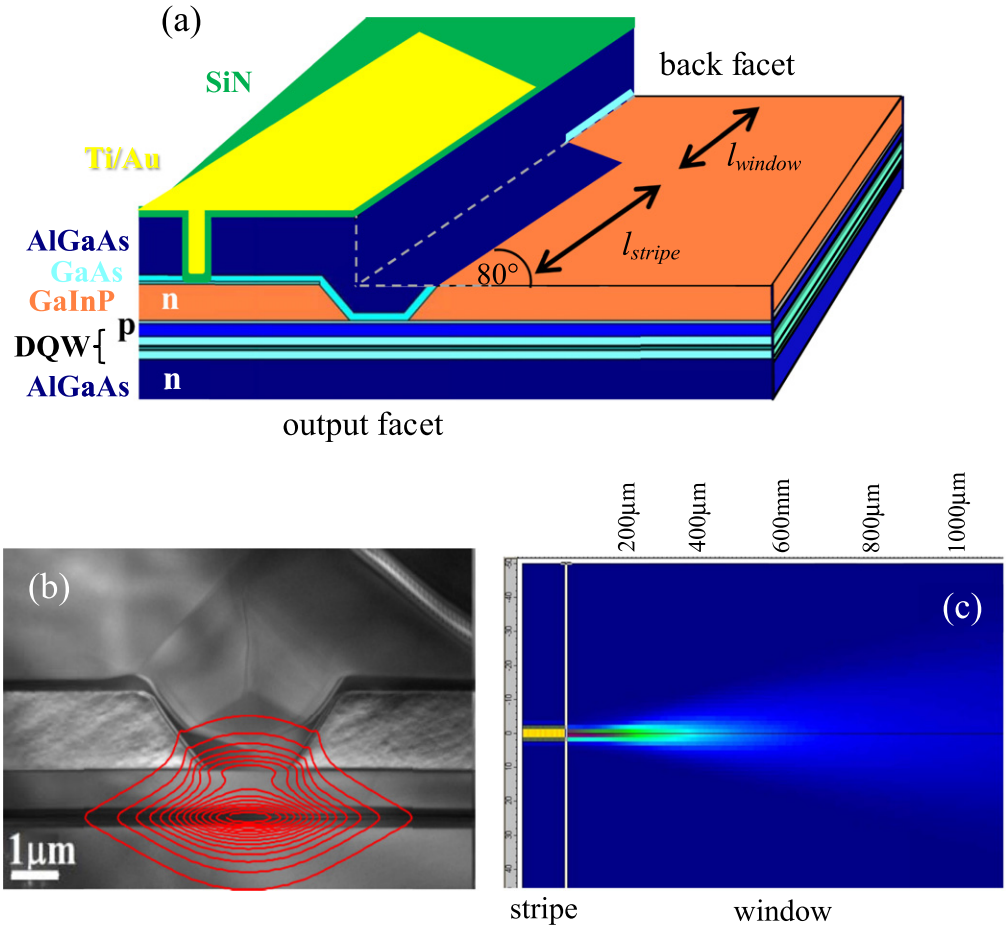

Figure 1. (a) Schematic diagram of the self-aligned stripe SLD with the overgrown cladding cut away from the right hand side to help identify the waveguide stripe, l_{stripe}, and window region, l_{window}. A TEM cross-section through the active stripe of this device is shown in (b). The position of the optical mode with respect to the waveguide is superimposed upon the TEM for illustration. (c) A simulated plan view optical mode profile to illustrate the spreading of light in the window region.

and tilted waveguides to offer R_{eff} below 10^{-5} [3]. Furthermore, the use of absorbing sections to reduce R_{eff} below 10^{-6} has been shown, using bent passive absorbers [4, 5], or grounded absorbers [6]. With respect to ridge waveguide approaches, buried ridge or stripe methods allow for narrow active widths and control of carrier flow, reduced non-radiative recombination at exposed surfaces, and greater control of the optical beam profile allowing for improved coupling to fibre.

Biological applications require light penetration into highly turbid and absorbing tissue. The range of near-IR wavelengths accessed by GaAs based devices is ideally suited to this biological band [7]. Typically, GaAs-based SLDs are realised using a combination of AR coatings and tilted facets. In addition, etched deflectors and long tapered absorbers have been demonstrated [8]. However, only a limited number of reports have been made regarding window facets on GaAs devices. Window devices are commonplace on InP [9]. However, it is difficult to directly transfer the window facet concept to GaAs due to the use of AlGaAs waveguide cladding and the requirement for regrowth upon exposed aluminium-containing layers in order to produce a buried waveguide. The application of window facets on GaAs has mainly been limited to non-interacting facets for raising the catastrophic optical damage threshold in high-power lasers [10], or have been realised using processes where aluminium-containing layers are exposed prior to overgrowth of the transparent window [11, 12]. Such processes raise concerns over the long-term reliability of a growth interface on oxidised AlGaAs. Furthermore, alternative solutions comprising GaInP cladding lack design flexibility due to the limited range for which stoichiometry can be tailored and the smaller conduction band offset compared to AlGaAs cladding.

In this paper we present a new scheme for low R_{eff} facets, based on the application of a self-aligned stripe regrowth process [13], to realise window-like structures in GaAs-based SLDs. We demonstrate low SMD from SLDs with no facet coating, making them naturally broadband. Our self-aligned stripe technology consists of a two-stage growth sequence in which GaAs/AlGaAs cladding layers are regrown upon a patterned GaInP optoelectronic confinement layer to form the structure shown schematically in figure 1(a), which provides both optical and electrical confinement. A transmission electron micrograph (TEM) is shown in (b), taken through the active stripe of this device. The position of the optical mode with respect to the waveguide is superimposed upon the TEM

for illustration. By terminating the waveguide prior to the cleaved back facet, light is allowed to spread in the laterally unguided window region. However, in contrast to traditional optically transparent window structures, the active region remains intact below the opto-electronic confining GaInP layer. Therefore light also undergoes absorption within the window-like region, resulting in further suppression of feedback into the waveguide and correspondingly lower R_{eff}. A plan view optical mode profile, simulated using FIMMPROP by Photon Design, is shown in figure 1(c) to illustrate the spreading of light in the window region.

The contrast between the modal refractive index in the stripe (3.284) and in the window region (3.281), calculated using FIMMWAVE by Photon Design, indicate $R_{\text{eff}} \sim 10^{-7}$, applying Snell's law for a plane wave incident upon an abrupt interface. However, the real interface is not abrupt due to the angled regrowth interface resulting from the GaInP wet etch, which is expected to reduce this effective reflectivity. Furthermore, this simple approximation does not take into account the competing dependences of refractive index on carrier density and self-heating during operation.

A waveguide structure was grown based on that described previously [13], containing two 7.6 nm $In_{0.17}Ga_{0.83}As$ QWs separated by 10 nm $GaAs_{0.9}P_{0.1}$ strain balancing layers, and 50 nm GaAs at either side forming the waveguide core. This core was grown within n-doped $Al_{0.42}Ga_{0.58}As$ lower cladding and 300 nm p-doped $Al_{0.42}Ga_{0.58}As$. 20 nm GaAs was grown prior to 600 nm n-doped GaInP, lattice matched to GaAs, and finally 15 nm GaAs. 3 μm wide self-aligned stripes were patterned 10° off from the normal to the crystal axis using standard UV photolithography and etched via a combination of dry and highly selective wet chemical etching using H_3PO_4 and HCl, stopping abruptly at the GaAs immediately below the GaInP layer. Samples were cleaned and returned to the MOVPE reactor for overgrowth of 100 nm p-doped GaAs, 1500 nm p-doped $Al_{0.42}GaAs$, 200 nm p-doped GaAs. Electrical isolation trenches were etched down to the GaInP layer at either side of the stripe, continuing throughout the entire length of the structure to create 100 μm wide electrically isolated devices. Au/Zn/Au ohmic contacts were deposited above the waveguide stripe and annealed before a SiN layer was deposited and a window etched above the stripe to allow use of TiAu bondpads. These were deposited, before the substrate was thinned and a back InGe/Au contact deposited and annealed. Cleaved SLDs were mounted with AuSn epi-side down upon AlN tiles, and tested at room temperature. The SLDs have windows at one end (back facet) and the output is collected from the waveguided front facet.

It is possible to ascertain the R_{eff} of our window-like SLD structure through a study of the threshold current density, J_{th}, of standard Fabry–Perot lasers, as a function of increasing window length. First, construction of a plot of gain, G, versus current density, J, allows extraction of G_{o} and J_{o}. The G–J curve is shown in figure 2(a), with upper and lower bounds to the data providing a range of possible G_o values. Our extrapolation to high current density does not take into account nonlinearity of G–J relations such as spectral and spatial hole burning [14], since we assume these to be low in SLDs compared with lasers. Next, 1 mm long stripe waveguides with varying window section lengths (0–2.25 mm) were processed normal to the cleaved facet and J_{th} was recorded for devices as a function of increasing window length, l, until the point at which lasing could no longer be achieved. Using these values of J_{th}, conversion into G_{th} allows an excess loss resulting from the window, α, to be calculated as the windowed G_{th}—laser G_{th}. R_{eff} is then determined from $R_{\text{cl}}e^{\alpha l}$, where R_{cl} is the reflectivity of the cleaved facet. R_{eff} is plotted as a function of window length in figure 2(b). We can therefore conservatively suggest that R_{eff} reaches $<10^{-11}$ at a window length of 2.25 mm. Tilting the waveguide with respect to the crystal axis can be expected to reduce R_{eff} further. We note that at these very small values, the reflectivity of the transition region between the stripe and window-region may dominate in producing ripple and parasitic lasing.

For an ideal SLD (0% facet reflectivity and no self-heating) the output power can be related to the gain (G) and active length (L) as shown in equation (1) [15]. This describes an exponential dependence of power on gain, as demonstrated in figure 3(a) for typical values of modal gain

$$P \propto \frac{(e^{GL} - 1)}{G}. \tag{1}$$

The spectral modulation observed within the electroluminescence (EL) spectrum of a SLD is defined [16] as [(peak-valley)/(peak + valley)]. Gain can be extracted from the modulation (peak/valley ratio) in the sub-threshold EL spectrum using the Hakki–Paoli equation [17]. From the definition of the SMD and the modulation, SMD can be related to gain as:

$$\text{SMD} \propto \left(\frac{e^{-GL} + R}{e^{-GL} - R}\right)^2. \tag{2}$$

By fixing the reflectivity (R) at 4×10^{-7} (R_{rear} is taken from the results in figure 2 and R_{front} was set to 1×10^{-4}, a typical R_{eff} for a tilted facet), SMD can be plotted as a function of gain for devices with three different active stripe lengths, as shown in figure 3(b). Since the power and SMD are both functions of the modal gain, from the equations (1) and (2), SMD can be plotted as a function of output power as shown in figure 3(c). This almost linear relation is in agreement with experiments made by Kwong *et al* [11] in the regime of low R_{eff}, using devices with an AR coating and a grounded internal absorber. The gradient in figure 3(c) is observed to reduce with increasing cavity length. This means that longer cavity length is beneficial in reducing SMD for a given output power. It should be noted that it is impractical to greatly increase the chip length since threshold gain is inversely proportional to cavity length, and both the drive current and the material real estate used become unfeasibly large.

In order to demonstrate the relative performance of SLDs with different stripe lengths, the characteristics of SLDs with

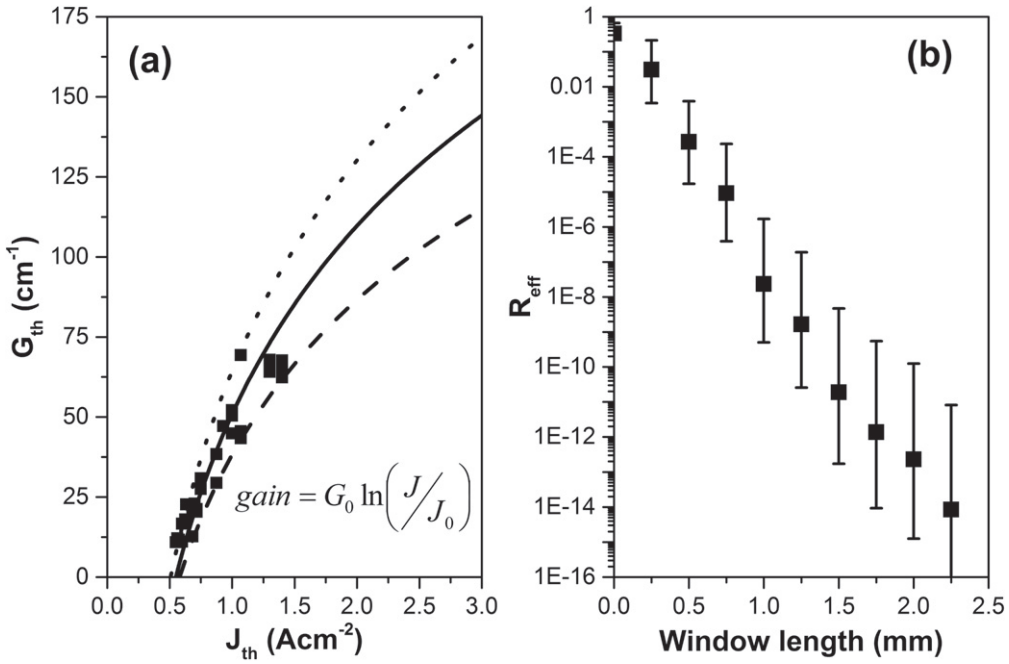

Figure 2. (a) *G*–*J* curve recorded from different length lasers. Upper and lower bounds are fit using $G_o = 70\ \text{cm}^{-1}$ (dashed) and $95\ \text{cm}^{-1}$ (dotted). Effective reflectivity, R_{eff}, is plotted as a function of window length in (b) for $G_o = 85\ \text{cm}^{-1}$, with error bars associated with using G_o as $70\ \text{cm}^{-1}$ (upper) and $95\ \text{cm}^{-1}$ (lower).

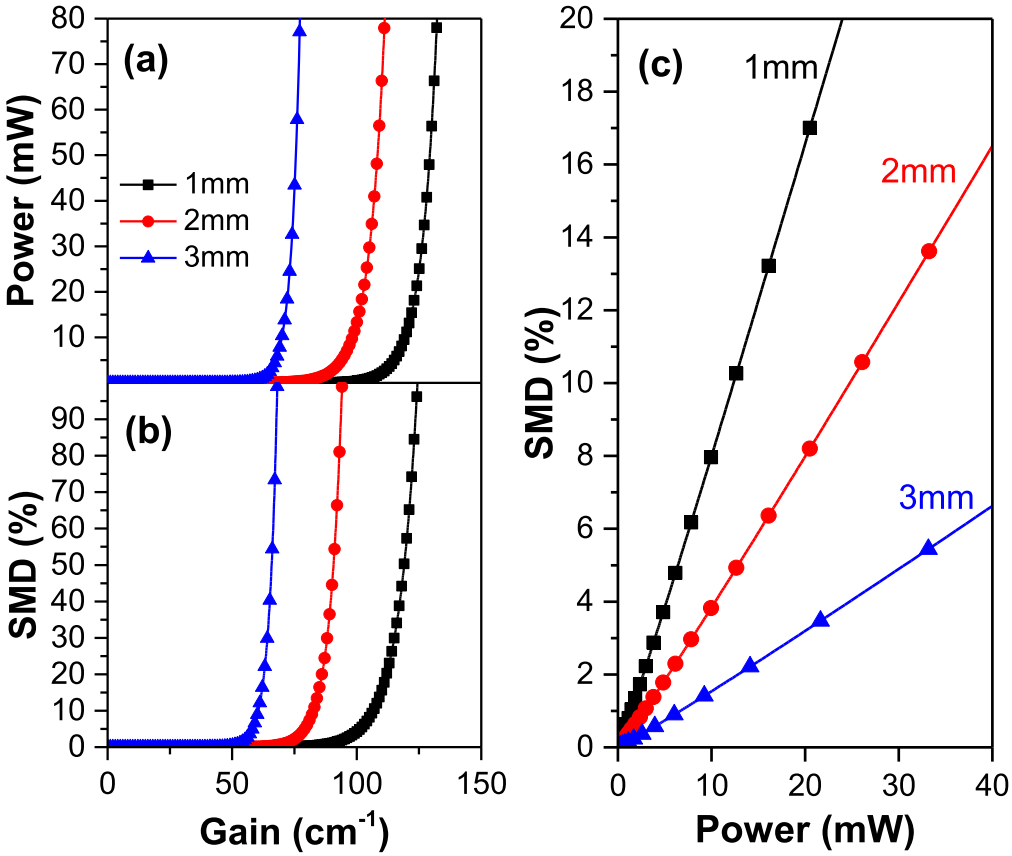

Figure 3. (a) Simulated power, and (b) spectral modulation depth, as functions of gain for 1, 2 and 3 mm active stripe lengths. (c) Plots the corresponding SMD as a function of power.

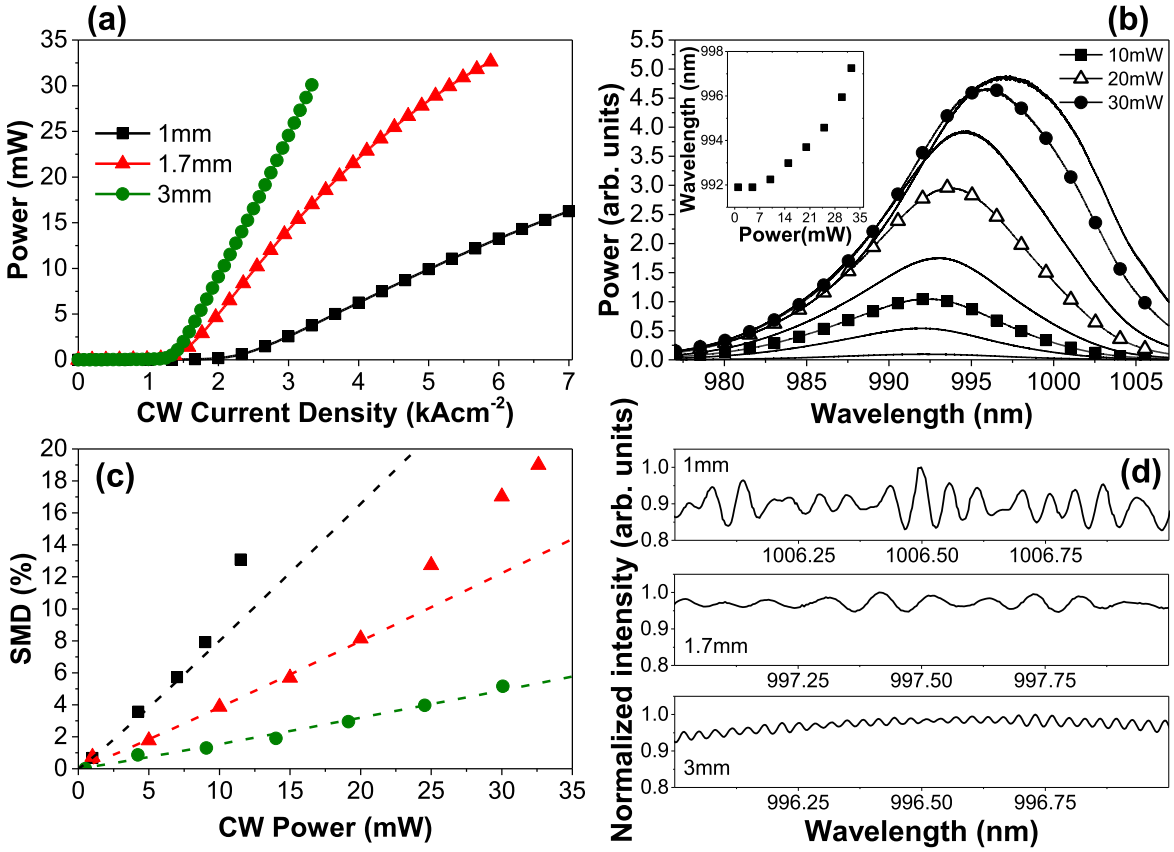

Figure 4. (a) Power as a function of current density for SLDs with three different geometries, (b) corresponding low resolution EL spectral evolution from the 1.7 mm long SLD up to 32.6 mW, with the peak wavelength as a function of CW output power in the inset. (c) Plots SMD versus CW output power for the three devices (the dotted lines represent the fit to the experimental data) and (d) plots the high resolution spectra for the three SLDs on the same scale, normalised to maximum power, measured at 10 mW output power.

three different geometries (1 mm with 1 mm window, 1.7 mm with 0.7 mm window and 3 mm with 2 mm window) are compared in figure 4. Comparison of SLDs with comparable stripe length (1.7 mm) but different window lengths (0.7 and 1.2 mm, not shown) revealed no measurable difference in performance, effectively decoupling the effects of stripe and window length at these long window lengths. Figure 4(a) plots the output power as a function of current density for the three SLDs. Lasing is supressed up to the maximum powers shown.

High resolution EL spectra were recorded using an Advantest Q8384 optical spectrum analyser with 0.01 nm resolution. A mode spacing of 0.08 nm allows accurate determination of the peak and valley intensities within the spectrum. This mode spacing is consistent with the length of the active stripe, corresponding to reflection at the stripe/window interface. Figure 4(b) plots the evolution of the EL spectrum of the 1.7 mm long SLD, recorded at a lower resolution of 0.1 nm from 1 to 30 mW, for clarity. The peak emission wavelength of the 1.7 mm long SLD is plotted in the inset to figure 4(b) as a function of its output power, from 1 to 32.6 mW. At high current densities the central wavelength of the emission spectrum is observed to red-shift by ~6 nm away from the low current peak when ~6 kA cm^{-2} is injected, as a result of Joule heating in the device under continuous wave operation.

A plot of SMD as a function of output power is constructed in figure 4(c) from high resolution spectra, together with fits to the data as shown by the dotted lines. A small section of high resolution spectra, recorded at 10 mW output power, are shown in figure 4(d). The SMD is seen to increase with increasing power for all stripe lengths, with a smaller gradient for larger stripe lengths, consistent with the prediction in figure 3(c). It is possible to fit the data in figure 4(c) only at low current. However, at high current, an abrupt deviation occurs.

Absorption in the window-like region of our SLD is beneficial in attaining such low R_{eff}. At low current densities (corresponding to low output powers) light travelling from the active stripe through the window region will be absorbed, contributing to the very low SMD. As observed in figure 4(b), at higher current densities self-heating in the active stripe results in a red-shift of emission. Meanwhile, non-ideal heat spreading in the buried stripe means that the unpumped window region probably operates at a cooler temperature, and the SLD emission peak shifts to the longer side of the absorption peak. The lower absorption available at these longer wavelengths may therefore permit light to travel

through the window, which becomes increasingly transparent with increasing current density.

This mechanism can be linked to the behaviour observed in figure 4(c), in which two fits are necessary to the SMD versus power curve for the SLD with 1.7 mm stripe length, with differing rear facet R_{eff}—one for powers <20 mW and another for powers >20 mW, corresponding to two different values of R_{eff} in the simulation. Below 20 mW the central emission wavelength is still coincident with the absorption peak in the window, while at higher powers the central wavelength is red-shifted to about 998.5 where the absorption is clearly reduced. Here, the measured SMD value is better fit by a line calculated using a larger R_{eff}. At the same time, the period of the highest spectral modulation is observed to change from 0.074 nm at 5 mW output power to 0.06 nm at 32.6 mW, consistent with a change in the dominant feedback cavity from reflection at the interface to reflection at the end facet for longer wavelengths $\geqslant$1000 nm. At shorter wavelengths the mode spacing remains at 0.074 nm.

Higher power SLDs have been reported, such as 1.3 W [8] but are based on measurement of broad area devices as opposed to the narrow stripe reported here. At this point in time, commercially available SLDs based on similar active widths demonstrate similar performance (power and spectral modulation) to that reported here. Our approach therefore offers comparable performance, but avoids the need for application of AR coatings, which will be beneficial in the pursuit of broader bandwidth SLDs. Alternatively, ultra-low ripple is possible via facet coating in future. Furthermore, it is anticipated that such a high level of feedback suppression could allow waveguides to be processed parallel to the crystal axis. Using such normal-facet approaches will allow a smaller chip size and improved beam quality (and hence fibre-coupling efficiency) as compared to tilted waveguides.

Conclusion

We have demonstrated a GaAs-based SLD based on a self-aligned stripe process with incorporation of a window-like back facet for attainment of low R_{eff} over a broad bandwidth, without application of facet coatings. This has resulted in realisation of high power (>30 mW) and low SMD (<5%) SLDs. Design criteria for high power and low SMD have been discussed, with longer length SLDs offering lower SMD to higher powers.

Acknowledgments

The authors gratefully acknowledge research grants provided by the UK Engineering & Physical Sciences Research Council (EPSRC), references EP/J004898/1 and EP/I018328/1.

References

[1] Drexler W and Fujimoto J 2008 *Optical Coherence Tomography: Technology and Application* (Berlin: Springer)
[2] Cha I, Kitamura M and Mito I 1989 1.5 μm band travelling-wave semiconductor optical amplifiers with window facet structure *Electron. Lett.* **25** 242
[3] Connelly M J 2004 *Semiconductor Optical Amplifiers* (Boston: Klewer Academic Publishers)
[4] Fu L, Schweizer H, Zhang Y, Li L, Baechle A, Jochum S, Bernatz G C and Hansmann S 2004 Design and realization of high-power ripple-free superluminescent diodes at 1300 nm *IEEE J. Quantum Electron.* **40** 1270
[5] Nagai H, Noguchi Y and Sudo S 1989 High-power, high-efficiency 1.3 μm superluminescent diode with a buried bent absorbing guide structure *Appl. Phys. Lett.* **54** 1719
[6] Semenov A T, Shidlovski V R, Safin S A, Konyaev V P and Zverkov M V 1993 Superluminescent diodes for visible (670 nm) spectral range based on AlGaInP/GaInP heterostructures with tapered grounded absorber *Electron. Lett.* **29** 530
[7] Profio A E and Doiron D R 1987 Transport of light in tissue in photodynamic therapy of cancer *Photochem. Photobiol.* **46** 591
[8] Burrow L, Causa F and Sharma J 2005 Ripple-free superluminescent diode *IEEE Photonics Technol. Lett.* **17** 2035–7
[9] Kashima Y, Matoba A and Takano H 1992 Performance and reliability of InGaAsP superluminescent diode *J. Lightwave Technol.* **10** 1644–9
[10] Matsumoto M, Sasaki K, Kondo M, Ishizumi T, Takeoka T, Nakatsu H, Watanabe M, Yamamoto O and Yamamoto S 1993 High-power 780 nm AlGaAs narrow-stripe window structure lasers with window grown on facets *Japan. J. Appl. Phys.* **32** 665–7
[11] Kwong N S K, Lau K Y and Bar-Chaim N 1989 High-power high-efficiency GaAlAs superluminescent diodes with an internal absorber for lasing suppression *IEEE J. Quantum Electron.* **25** 696–704
[12] Tateoka K, Naito H, Yuri M, Kume M, Hamada K, Shimizu H, Kazumura M and Teramoto I 1991 A high-power GaAlAs superluminescent diode with an antireflective window structure *IEEE J. Quantum Electron.* **27** 1568–73
[13] Groom K M, Alexander R R, Childs D T D, Krysa A B, Roberts J S, Helmy A S and Hogg R A 2008 GaAs-based self-aligned laser incorporating InGaP opto-electronic confinement layer *Electron. Lett.* **44** 905–6
[14] Vasil'ev P 1995 *Ultrafast Diode Lasers, Fundamentals and Applications* (Boston, MA: Artech House)
[15] Suhara T 2004 *Semiconductor Laser Fundamentals* (New York: Marcel Dekker)
[16] Zhang Z Y, Wang Z G, Xu B, Jin P, Sun Z Z and Liu F Q 2004 High-performance quantum-dot superluminescent diodes *IEEE Photonics Technol. Lett.* **16** 27
[17] Hakki B W and Paoli T L 1975 Gain spectra in GaAs double-heterostructure injection lasers *J. Appl. Phys.* **46** 1299–306